ISBN: 978-3-95450-261-5 ISSN: 2673-7000 doi: 10.18429/JACoW-NAPAC2025-WEP073

# PROGRESS UPDATE ON COMPRESSED ULTRASHORT PULSE INJECTOR DEMONSTRATOR

W. H. Tan*, A. Dhar, J. Hernandez, E. A. Nanni
SLAC National Accelerator Laboratory, Menlo Park, CA, USA

*Abstract*

Stable high gradient operation of a photoinjector is important for generating high brightness electron beams. The Argonne Wakefield Accelerator (AWA) facility recently commissioned an X-band photoinjector at 400 MV/m cathode field without significant breakdown rates using nanosecond RF pulses generated from a wakefield accelerator. We propose to develop an X-band photoinjector at 500 MV/m cathode field fed by ultrashort RF pulses generated by RF pulse compression technology developed at SLAC National Accelerator Laboratory, named as Compressed Ultrashort Pulse Injector Demonstrator (CUPID). The klystron based pulse compression is more stable and allows higher repetition rate. Here we provides the progress update of CUPID project, in particular on the mechanical design of the electron gun, solenoid's requirement and design constraints.

## INTRODUCTION

The invention of photoinjector enabled the generation of high brightness electron beams, where photoemitted electrons are accelerated to high energies by a radiofrequency electron gun to suppress the degradation of beams' brightness due to charge repulsion [1, 2]. High brightness electron beams are important for accelerator-based applications, where the two most notable ones are being the free-electron-lasers (FELs) and electron microscopy [3].

The quality of an electron beam is given by its six-dimensional brightness, $\mathcal{B}_{6D} = 2I/\varepsilon_n^2\sigma_\gamma$, where $I$, $\varepsilon_n$ and $\sigma_\gamma$ are the beam current, transverse emittance and normalized rms energy spread respectively [4]. High accelerating gradient at the cathode can achieve bright electron beams since the brightness is proportional to the square of the applied field at the cathode, but comes with RF breakdowns $\mathcal{B}_{6D} \propto E^2$ [4–11]. One possible way to achieve high gradient is to reduce the time duration of the feeding in RF pulses since phenomenological studies showed that the breakdown rate is proportional to the applied field gradient but inversely proportional to the RF pulse duration [12]. The Argonne Wakefield Accelerator (AWA) achieved high gradient at ~400 MV/m without significant breakdowns on an X-band 11.7 GHz gun [13]. AWA achieved this by using a wakefield accelerator that accelerates 400 nC electron bunches to high energies and generates ~10 ns high power RF pulses from a power-extraction-and-transfer structure (PETS) [14].

We propose to develop Compressed Ultrashort Pulse Injector Demonstrator (CUPID), a 1.6 cell electron gun that can achieve high gradient with ultrashort high power RF pulses generated by a RF pulse compressor at 11.424 GHz to utilize the available X-band klystrons of the same frequency and a RF pulse compressor at SLAC [15]. In this paper, we discuss the design of the CUPID electron gun, the solenoid's requirement, design constraints and preliminary beam dynamics studies.

* whtan@slac.stanford.edu

## CUPID GUN DESIGN

The CUPID electron gun is designed to operate at 500 MV/m at the cathode fed by a 300 MW, 10 ns RF pulse. This is achieved by designing the electron gun to operate in the transient regime where RF pulses fill the gun quickly and reflect back. The exit of the CUPID gun is modeled as a 11.43 mm waveguide to connect to an available $TM_{01}$ X-band mode launcher [16, 17]. This allows us to have flexibility in reusing the existing mode launcher. Figure 1(a) shows the mechanical design of the CUPID gun with the attached $TM_{01}$ mode launcher and superimposed electric field map, all enclosed inside a solenoid. This mockup solenoid is designed to evaluate the physical dimensions needed for the full solenoid design. Figure 1(b) shows the zoomed-in view of CUPID gun and the mode launcher. Based on the current design, the solenoid needs to have a bore diameter larger than 70 mm diameter of the flange and a length shorter than 75 mm.

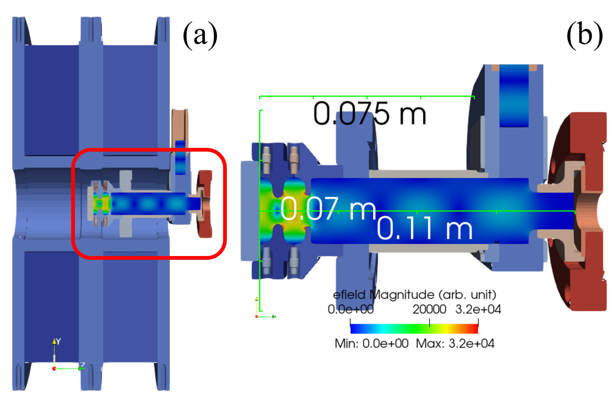


Figure 1: (a) The design of CUPID gun with an attached $TM_{01}$ mode launcher, its fieldmap and a mockup solenoid. (b) Zoomed-in view. The gun assembly has 70 mm diameter, 75 mm (110 mm) long before (after) the attached mode launcher.

Figure 2 shows the evolution of the beam energy at the on-crest phase. The beam energy out of the gun exit is 4.7 MeV. Since the CUPID gun is designed to operate in a transient regime, there are traveling waves present in the waveguide

ISBN: 978-3-95450-261-5 ISSN: 2673-7000 doi: 10.18429/JACoW-NAPAC2025-WEP073

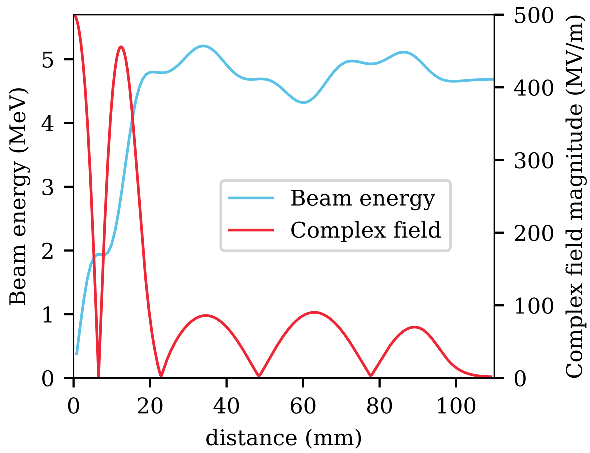


Figure 2: The evolution of beam energy at the on-crest phase. The beam experiences acceleration and deceleration after exiting the full cell at 20 mm due to the presence of traveling waves in the waveguide.

that connects the CUPID gun and the mode launcher. As the phase of traveling waves is not adjusted to synchronize with the beam's phase, the beam experiences both acceleration and deceleration. This is the design constraint that we chose for operating at the transient regime and using this particular waveguide coupler.

The solenoid for the CUPID gun is required to be very compact due to the design choices made. In particular, the bore diameter of the solenoid must be larger than the diameter of the connecting flange at 70 mm. The length of the solenoid needs to be shorter 75 mm, as imposed by the rectangular waveguide of the $TM_{01}$ mode launcher. These design choices allow us to reuse existing beamline components and give the flexibility of swapping different electron guns. Beam dynamics simulations were employed to study the requirement of solenoid in delivering low emittance beams, and provided feedback to revise the design of CUPID gun.

Table 1 summarizes the design parameters of CUPID gun, reproduced from [18].

Table 1: Design Parameters for the X-band Gun, reproduced from Ref. [18]

| **Parameter** | **Value** | **Unit** |
|---|---|---|
| Frequency | 11.424 | GHz |
| Loaded Q-factor | 215 | - |
| $S_{11}$ | −0.58 | dB |
| Field gradient at cathode | 500 | MV/m |
| RF pulse length | 10 | ns |

## BEAM DYNAMICS

We performed beam dynamics simulation studies with the CUPID gun to investigate its performance for delivering high brightness beams. In particular, we are interested in the generation of 100 nm emittance, 100 pC electron beams similar to the proposed upgrade of the upcoming LCLS-II HE photoinjector [19]. In our studies, the initial beam distribution has MTE of 400 meV, corresponds to the thermal emittance 0.9 µm/mm [20]. The beam is assumed to have a radial uniform and flat top temporal distribution.

Figure 3 shows two solenoid field profiles used for the beam dynamics studies. These field profiles were employed to investigate the feasibility of the compact mechanical design of CUPID gun with attached mode launcher. Solenoid 1 is numerically generated and fits within physical constraints, whereas Solenoid 2 does not fit the length requirement and is from the existing XTA beamline [9]. Beam dynamics studies were performed on two different photoinjector designs where both shares the CUPID gun and a 1 m long, 160 MV/m downstream S-band distributed-coupling linac, but differ in solenoid field profile [21]. Simulation studies were performed using the beam dynamics software ASTRA [22]. Our simulations used the cylindrically-symmetric space charge algorithm. Multi-objective optimizations were employed to study the performance of CUPID gun and two different solenoid profiles. The two objectives for the optimization studies are the six-dimensional brightness $\mathcal{B}_{6\mathrm{D}}$ and the transverse emittance $\varepsilon_n$.

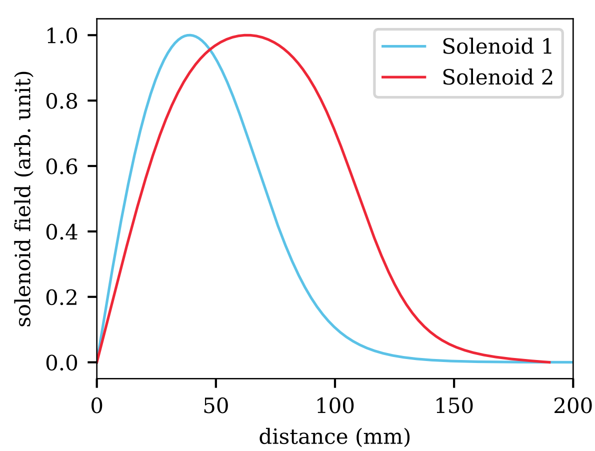


Figure 3: Two solenoid profiles were used for the beam dynamics studies to investigate the feasibility of the compact mechanical design of CUPID gun with attached mode launcher. Solenoid 1 is numerically generated and fits within the physical constraints, whereas Solenoid 2 is taken from the existing XTA beamline and does not fit the length requirement [9].

Figure 4 shows Pareto fronts of optimizations using two different solenoid field profiles. Solenoid 1 shows better performance than Solenoid 2 in delivering high brightness beams. Figure 5 shows the evolution of transverse emittance of these two solenoid profiles. Photoinjector based on Solenoid 1 requires the downstream linac at 0.4 m from the cathode, compared to 0.51 m of Solenoid 2. Overall,

ISBN: 978-3-95450-261-5 ISSN: 2673-7000 doi: 10.18429/JACoW-NAPAC2025-WEP073

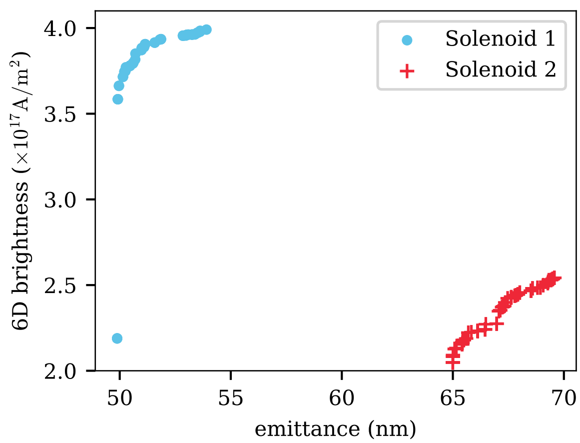


Figure 4: Pareto fronts of beam dynamics multi-objective optimizations with Solenoid 1 (blue) and Solenoid 2 (orange). The six-dimensional brightness $\mathcal{B}_{6D}$ and the transverse emittance $\varepsilon_n$ are the two objectives.

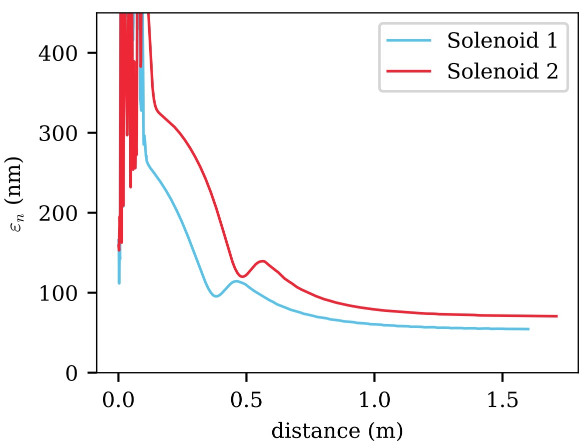


Figure 5: Example beam dynamics results with optimized parameters for Solenoid 1 (blue) and Solenoid 2 (orange). Solenoid 1 delivers low emittance beams but requires a stronger and shorter solenoid.

Solenoid 1 delivers better performance and more compact, but comes with the challenge of designing a high magnetic field, short solenoid. In addition to that, putting the downstream linac very close to the CUPID gun imposes additional challenge of designing incident laser system for photoemission. Table 2 summarizes differences in magnetic field strength, linac position and beam parameters for both solenoid designs.

## CONCLUSION

In summary, we present CUPID, a high gradient X-band electron gun operating at 11.424 GHz and 500 MV/m, fed by a 300 MW, 10 ns RF pulse. This is achieved by the pulse compression technology presented at SLAC. We show the current design of CUPID gun with attached $TM_{01}$ mode launcher. Our beam dynamics studies show that CUPID gun is capable of producing electron beams down to transverse emittance of 52 nm, and highlight the design challenge of the solenoid. We plan to reevaluate the feasibility of our current CUPID design and the technical challenge of the solenoid in our future studies.

Table 2: Optimized Parameters for the Injector and Generated Beam Parameters

| Parameter | Solenoid 1 | Solenoid 2 | Unit |
|---|---|---|---|
| Linac position | 0.4 | 0.51 | m |
| Solenoid field | 0.87 | 0.59 | T |
| Beam energy | 91 | 91 | MeV |
| Bunch length | 336 | 339 | µm |
| RMS size | 49 | 53 | µm |
| Emittance | 55 | 70 | nm |
| Energy spread | 0.27 | 0.27 | % |

## ACKNOWLEDGMENTS

This work is supported by the U.S. Department of Energy Contract No. DE-AC02-76SF00515 with SLAC National Accelerator Laboratory. Simulation works used resources of the National Energy Research Scientific Computing (NERSC) Center, U.S. Department of Energy Office of Science User Facility located at Lawrence Berkeley National Laboratory, operated under Contract No. DE-AC02-05CH11231.

## REFERENCES

[1] J. Fraser, R. Sheffield, E. Gray, and G. Rodenz, "High-brightness photoemitter injector for electron accelerators", *IEEE Trans. Nucl. Sci.*, vol. 32, no. 5, pp. 1791–1793, 1985. `doi:10.1109/TNS.1985.4333725`

[2] B. Carlsten, "New photoelectric injector design for the los alamos national laboratory xuv fel accelerator", *Nucl. Instrum. Methods Phys. Res. A: Accel. Spectrom. Detect. Assoc. Equip.*, vol. 285, no. 1, pp. 313–319, 1989. `doi:10.1016/0168-9002(89)90472-5`

[3] X. Wang, P. Musumeci, E. Lessner, and J. Goldstein, *Report of the Basic Energy Sciences Workshop on the Future of Electron Sources*. U.S. Department of Energy, 2016. `doi:10.2172/1616511`

[4] J. B. Rosenzweig *et al.*, "An ultra-compact x-ray free-electron laser", *New J. Phys.*, vol. 22, no. 9, p. 093 067, 2020. `doi:10.1088/1367-2630/abb16c`

[5] S. Döbert *et al.*, "High Power Test of an X-Band Slotted-iris Accelerator Structure at NLCTA", *Conf. Proc. C*, vol. 070625, p. 2191, 2007. `doi:10.1109/PAC.2007.4441193`

[6] F. Wang, "Breakdown characteristics study on an 18 cell X-band structure", *AIP Conf. Proc.*, vol. 1086, no. 1, pp. 373–379, 2009. `doi:10.1063/1.3080934`

ISBN: 978-3-95450-261-5 ISSN: 2673-7000 doi: 10.18429/JACoW-NAPAC2025-WEP073

[7] V. Dolgashev, S. Tantawi, Y. Higashi, and B. Spataro, "Geometric dependence of radio-frequency breakdown in normal conducting accelerating structures", *Appl. Phys. Lett.*, vol. 97, no. 17, p. 171 501, 2010. doi:10.1063/1.3505339

[8] L. Laurent *et al.*, "Experimental study of rf pulsed heating", *Phys. Rev. Spec. Top. Accel. Beams*, vol. 14, no. 4, p. 041 001, 2011. doi:10.1103/PhysRevSTAB.14.041001

[9] C. Limborg-Deprey *et al.*, "Performance of a first generation x-band photoelectron RF gun", *Phys. Rev. Accel. Beams*, vol. 19, no. 5, p. 053 401, 2016. doi:10.1103/PhysRevAccelBeams.19.053401

[10] R. A. Marsh, G. G. Anderson, S. G. Anderson, D. J. Gibson, C. P. J. Barty, and Y. Hwang, "Performance of a second generation X-band RF photoinjector", *Phys. Rev. Accel. Beams*, vol. 21, no. 7, p. 073 401, 2018. doi:10.1103/PhysRevAccelBeams.21.073401

[11] A. D. Cahill, J. B. Rosenzweig, V. A. Dolgashev, S. G. Tantawi, and S. Weathersby, "High gradient experiments with X-band cryogenic copper accelerating cavities", *Phys. Rev. Accel. Beams*, vol. 21, no. 10, p. 102 002, 2018. doi:10.1103/PhysRevAccelBeams.21.102002

[12] A. Grudiev, S. Calatroni, and W. Wuensch, "New local field quantity describing the high gradient limit of accelerating structures", *Phys. Rev. Spec. Top. Accel. Beams*, vol. 12, no. 10, p. 102 001, 2009. doi:10.1103/PhysRevSTAB.12.102001

[13] W. H. Tan *et al.*, "Demonstration of sub-GV/m accelerating field in a photoemission electron gun powered by nanosecond $X$-band radio-frequency pulses", *Phys. Rev. Accel. Beams*, vol. 25, no. 8, p. 083 402, 2022. doi:10.1103/PhysRevAccelBeams.25.083402

[14] M. Peng *et al.*, "Generation of High Power Short Rf Pulses using an X-Band Metallic Power Extractor Driven by High Charge Multi-Bunch Train", in *Proc. IPAC'19*, Melbourne, Australia, pp. 734–737, 2019. doi:10.18429/JACoW-IPAC2019-MOPRB069

[15] A. Dhar, M. Othman, and V. Dolgashev, "Development of ultra high power compact x-band pulse compressor", IPAC'25, Taipei, Taiwan, Jun. 2025, 2025. https://indico.jacow.org/event/81/contributions/8523

[16] M. Dal Forno, "Design of a high power $TM_{01}$ mode launcher optimized for manufacturing by milling", SLAC National Accelerator Lab., Tech. Rep. SLAC-PUB-16902, 2016. doi:10.2172/1336365

[17] G. Torrisi *et al.*, "Low power RF test of a quadrupole-free X-band mode launcher for high brightness applications", *J. Phys.: Conf. Ser.*, vol. 1350, no. 1, p. 012 188, 2019. doi:10.1088/1742-6596/1350/1/012188

[18] W. Tan *et al.*, "Compressed ultrashort pulse injector demonstrator", IPAC'25, Taipei, Taiwan, 2025. https://indico.jacow.org/event/81/contributions/7800

[19] F. Ji *et al.*, "Beam Dynamics Studies on a Low Emittance Injector for LCLS-II-HE", in *Proc. NAPAC'22*, Albuquerque, NM, USA, pp. 619–622, 2022. doi:10.18429/JACoW-NAPAC2022-WEPA02

[20] D. H. Dowell and J. F. Schmerge, "Quantum efficiency and thermal emittance of metal photocathodes", *Phys. Rev. Spec. Top. Accel. Beams*, vol. 12, no. 7, p. 074 201, 2009. doi:10.1103/PhysRevSTAB.12.074201

[21] A. Dhar *et al.*, "Distributed coupling linac for efficient acceleration of high charge electron bunches", in *Proc. IPAC'24*, Nashville, TN, pp. 1448–1450, 2024. doi:10.18429/JACoW-IPAC2024-TUPR14

[22] K. Floettmann, *ASTRA – A Space Charge Tracking Algorithm*. Deutsches Elektronen-Synchrotron, 2017. http://www.desy.de/%20mpyflo/